

**OFF-LINE ELECTRODES' EFFECT ON A
WENNER AND WENNER-SCHLUMBERGER
ARRAY USING TWO-DIMENSIONAL
ELECTRICAL RESISTIVITY TOMOGRAPHY**

MOHAMMED MUSTAPHA ADEJO

UNIVERSITI SAINS MALAYSIA

2021

**OFF-LINE ELECTRODES' EFFECT ON A
WENNER AND WENNER-SCHLUMBERGER
ARRAY USING TWO-DIMENSIONAL
ELECTRICAL RESISTIVITY TOMOGRAPHY**

by

MOHAMMED MUSTAPHA ADEJO

**Thesis submitted in fulfilment of the requirements
for the degree of
Doctor of Philosophy**

March 2021

ACKNOWLEDGEMENT

Foremost, I give all praise and adoration to Allah (SWT), the Omnipotent the Omniscience, for granting me good health, wisdom, patience and ability to complete this study. May the peace and blessings of Allah be upon our Nobel Prophet, Muhammad (SAW), his household and his companions. I would like to express my sincere gratitude to my supervisors, Professor Dr. Rosli Saad, Dr Nordiana Mohd Muztaza, and Dr Andy Anderson Bery for their guidance, time devotion, tireless encouragement and constant support throughout my study. It is indeed a great privilege to be mentored under their supervision. I shall remain ever grateful to them. Besides my supervisors, I would like to thank the internal and external examiners for their insightful comments and suggestions, which indeed added value to my thesis. My sincere thanks also go to the technical staff of the Geophysics Unit, Mr. Shahil Ahmad Khosani, Mr. Yaakub Othman (Rtd) and Mr. Zulkeflee Bin Ismail for their commitment and perseverance during the data acquisition.

I am grateful to all postgraduate colleagues of Geophysics, Universiti Sains Malaysia (USM), Mr. Bala Balarabe, Mr. John Adamu, Mr. Muhammad Nazrin, Mr. Mark Jinmin, Mr. Taquiuddin Zakaria, Mr. Usman Yaro, Mr. Abubakar Yusuf, Mr. Farid Rosli, Miss. Alyaa Nadhira, Miss. Nazirah, Dr. Adeeko Tajudden, Dr. Rais Yusoh, Dr. Kiu Yap Chong, Dr. Najmiah Rosli for their various contributions, ranging from providing constructive advice to data collection, and learning software applications. I would also like to particularly thank Mr. Haruna Abdu for his guide on the programming aspect of the thesis. In a special case, my sincere thanks goes to Dr. Muhammad Sabiu Bala, Dr. Fathi M. Abdullah, Dr. Ishola Kehinde Saheed, Dr. Nuraddeen Usman and Dr. Geraldine Anukwu for their immense guide.

My heartfelt appreciation goes to my family for their support, inspiration and encouragement. My lovely parents Mohammed Adejo and Salamatu Adamu, my lovely sister Zainab Muhammad and also my dearest cousins Engr. Salisu Salihu Shuaibu and Shafi`u Shauibu. I thank you all. My apology to friends and well-wishers whose name could not be mention, I cherish you all with silent gratitude. I deeply appreciate, and remain indebted to my darling wife Hadiza Ibrahim for her support, understanding and patience to be away from her (lonely) during my studies.

Finally, I would like to thank my employer, Federal University of Lafia, Nigeria, for granting me the opportunity and sponsorship in pursuit of this laudable program through the Tertiary Education Trust Fund (TetFund).

TABLE OF CONTENTS

ACKNOWLEDGEMENT	ii
TABLE OF CONTENTS	iv
LIST OF TABLES	viii
LIST OF FIGURES	x
LIST OF SYMBOLS	xv
LIST OF ABBREVIATIONS	xvii
ABSTRAK	xx
ABSTRACT	xxii
CHAPTER 1 INTRODUCTION	1
1.1 Background	1
1.2 Problem statements	4
1.3 Research objectives	5
1.4 Scope of study	5
1.5 Significance and novelty of the study	6
1.6 Thesis layout	6
CHAPTER 2 LITERATURE REVIEW	9
2.1 Introduction	9
2.2 The basic theory of the resistivity method	10
2.3 Concept of 2-D electrical resistivity tomography	17
2.3.1 Wenner array	20
2.3.2 Schlumberger array	21
2.3.3 Wenner-Schlumberger array	22
2.4 Measurement error in 2-D ERT survey	23
2.5 Evaluation of electrode arrays efficiency	25
2.6 Development of template/protocol for 2-D ERT survey	26

2.7	Chapter Summary.....	41
CHAPTER 3		
METHODOLOGY.....		42
3.1	Introduction	42
3.2	Research flow chart.....	42
3.3	Data acquisition.....	44
3.3.1	Wenner array with all electrodes inline (WN-AEI).....	44
3.3.2	Wenner array with offline electrodes arrangement.....	45
3.3.2(a)	Case I: Wenner array with one electrode offline (WN-1EO)	46
3.3.2(b)	Case II: Wenner array with two electrodes offline (WN-2EO)	47
3.3.2(c)	Case III: Wenner array with three electrodes offline (WN-3EO)	49
3.3.3	Wenner-Schlumberger array with all electrodes inline (WNS-AEI)	50
3.3.4	Wenner-Schlumberger array with electrodes offline.....	51
3.3.4(a)	Case I: Wenner-Schlumberger array with one electrode offline (WNS-1EO).....	51
3.3.4(b)	Case II Wenner-Schlumberger array with two electrodes offline (WNS-2EO).....	52
3.3.4(c)	Case III Wenner-Schlumberger array with three offline electrodes (WNS-3EO)	53
3.4	Data processing	54
3.4.1	Wenner array.....	54
3.4.2	Wenner-Schlumberger	57
3.5	Development of the processing template for Wenner and Wenner-Schlumberger array	59
3.6	Numerical accuracy assessment.....	62
3.6.1	Pearson's correlation coefficient (PCC)	63
3.6.2	Absolute error (AB), Mean absolute error (MAE) and Mean absolute percentage error (MAPE).....	64

3.7	Location and geology of the study area.....	65
3.8	Chapter summary	66
CHAPTER 4 RESULTS AND DISCUSSION		67
4.1	Introduction	67
4.2	Wenner array survey	67
4.2.1	Wenner array with all electrodes inline (WN-AEI) using the conventional program	68
4.2.2	Wenner array with electrodes offline.....	68
4.2.2(a)	Wenner array with one electrode offline (WN-1EO) using the conventional program.....	69
4.2.2(b)	Wenner array with two electrodes offline (WN-2EO) using the conventional program	71
4.2.2(c)	Wenner array with three electrodes offline (WN-3EO) using the conventional program	72
4.2.2(d)	Quantitative assessment of Wenner array with inline and offline electrode(s) using the conventional program	75
4.3	Wenner-Schlumberger array	77
4.3.1	Wenner-Schlumberger array with all electrodes inline (WNS-AEI) using the conventional program.....	77
4.3.2	Wenner-Schlumberger array with offline electrodes	78
4.3.2(a)	Wenner-Schlumberger with one electrode offline (WNS-1EO) using the conventional program	79
4.3.2(b)	Wenner-Schlumberger with two electrodes offline (WNS-2EO) using the conventional program	81
4.3.2(c)	Wenner-Schlumberger with three electrodes offline (WNS-3EO) using the conventional program.....	83
4.3.2(d)	Quantitative assessment of Wenner-Schlumberger (WNS) array with the inline and offline electrode(s) using the conventional program.....	85
4.4	Resistivity data processing template	87
4.5	Evaluation of the innovative template.....	89
4.5.1	Wenner array with one electrode offline (WN-1EO) using the innovative template	89

4.5.2	Wenner array with two electrodes offline (WN-2EO) using the innovative template	91
4.5.3	Wenner array with three electrodes offline (WN-3EO) using the innovative template	92
4.5.4	Quantitative assessment of Wenner array with the inline and offline electrode(s) using the innovative template.....	93
4.5.5	Wenner-Schlumberger with one electrode offline (WNS-1EO) using the innovative template	95
4.5.6	Wenner-Schlumberger with two electrodes offline (WNS-2EO) using the innovative template	97
4.5.7	Wenner-Schlumberger with three electrodes offline (WNS-3EO) using the innovative template	99
4.5.8	Quantitative assessment of Wenner-Schlumberger array with the inline and offline electrode(s) using the innovative template	100
4.5.9	Comparative assessment between Wenner and Wenner-Schlumberger arrays using the conventional program and innovative template.....	103
4.6	Chapter summary	106
CHAPTER 5 CONCLUSION AND RECOMMENDATIONS		107
5.1	Introduction	107
5.2	Conclusion.....	107
5.3	Recommendations for Future Research	109
REFERENCES.....		110
APPENDICES		
LIST OF PUBLICATIONS		

LIST OF TABLES

	Page
Table 3.1	Rule of thumb for interpreting the strength of a correlation coefficient (Mukaka, 2012).....64
Table 4.1	Summary of Pearson’s correlation coefficient between the true and the estimated models for Wenner array using the conventional program76
Table 4.2	Summary of mean absolute error between the true and the estimated models for Wenner array using the conventional program76
Table 4.3	Summary of mean absolute percentage error between the true and the estimated model Wenner array using the conventional program77
Table 4.4	Summary of Pearson’s correlation coefficient between the true and the estimated models for Wenner-Schlumberger array using the conventional program.....86
Table 4.5	Summary of mean absolute error between the true and the estimated models for Wenner-Schlumberger array using the conventional program.....86
Table 4.6	Summary of mean absolute error between the true and the estimated models for Wenner-Schlumberger array using conventional program.....87
Table 4.7	Summary of Pearson’s correlation coefficient between the true and the estimated models for Wenner array using the innovative template94
Table 4.8	Summary of mean absolute error between the true and the estimated models for Wenner array using the innovative template ...95

Table 4.9	Summary of mean absolute percentage error between the true and the estimated models for Wenner array using the innovative template	95
Table 4.10	Summary of Pearson’s correlation coefficient between the true and the estimated models for Wenner-Schlumberger array using the innovative template	101
Table 4.11	Summary of mean absolute error between the true and the estimated models for Wenner-Schlumberger array using the innovative template	102
Table 4.12	Summary of mean absolute error between the true and the estimated models for Wenner-Schlumberger array using the innovative template	102
Table 4.13	Summary of all the quantitative result for both arrays using conventional program and Innovative template	105

LIST OF FIGURES

	Page
Figure 2.1 Resistivity value of some common Earth materials (Palacky, 1987)	10
Figure 2.2 Current flow a single-point current electrode (Modified from Kearey et al., 2002)	12
Figure 2.3 Current lines and equipotential surfaces produced by a current source and sink (modified from (Lowrie, 2007)	14
Figure 2.4 The general form of an electrode configuration for resistivity measurement (modified from Reynolds, 2011)	14
Figure 2.5 Electrode arrangement in a multi-electrode system for a 2-D resistivity survey and the measurement sequence used to construct a 2-D pseudo-section (Loke et al., 2013)	19
Figure 2.6 Electrodes arrangement for Wenner array	20
Figure 2.7 Electrodes arrangement for Schlumberger array.....	22
Figure 2.8 Electrodes arrangement for Wenner-Schlumberger array.....	23
Figure 2.9 Position of the ERT profile lines, monitoring wells and boreholes (Liao et al., 2018).....	28
Figure 2.10 Location map of observation wells, ERT survey, and geology map of Sameerwadi watershed (Rao et al., 2014).....	29
Figure 2.11 Location map of Twarja river basin, with the locations of electrical resistivity tomography sites represented by the red circle (Rai et al., 2015).....	31
Figure 2.12 Gridding for the measuring points (white stripes show first 13 profile lines, and red dashed lines show the additional three profile lines) (Karavul et al., 2016).....	35
Figure 2.13 Survey lines of 2-D resistivity method at Lembah Bujang, Kedah (Saad et al., 2014).....	37

Figure 3.1	Research flow chart.....	43
Figure 3.2	Site photos for a 2-D electrical resistivity tomography survey with all electrodes inline	45
Figure 3.3 (a)	Site photos for a 2-D electrical resistivity tomography survey with electrode number 21 offline at 1.0 m distance (b) Affected data point in Wenner array with one offline electrode	47
Figure 3.4	(a) Site photos for a 2-D electrical resistivity tomography survey with electrode number 3 and 35 offline at 1.0 m distance (b) Affected data point in Wenner array with two offline electrode	49
Figure 3.5	(a) Site photos for a 2-D electrical resistivity tomography survey with electrode number 1, 21 and 31 offline at 1.0 m distance (b) Affected data point in Wenner array with three offline electrodes	50
Figure 3.6	Affected data point in Wenner-Schlumberger array with one offline electrode	52
Figure 3.7	Affected data point in Wenner-Schlumberger array with two offline electrodes.....	53
Figure 3.8	Affected data point in Wenner-Schlumberger array with three offline electrodes.....	53
Figure 3.9	Typical scenario of Wenner array with inline (blue circle) and offline (green circle) electrode arrangement (from top view).....	55
Figure 3.10	Typical scenario of Wenner-Schlumberger array with inline and offline electrode arrangement (from top view)	57
Figure 3.11	ABEM multi-purpose file format (*.AMP) for Wenner array	60
Figure 3.12	Processing template for (a) Wenner array (b) Wenner-Schlumberger array with non-collinear electrode arrangement	62
Figure 3.13	Geology map of Penang Island Malaysia (Modified from Pradhan & Lee, 2010)	66
Figure 4.1	Two-dimensional resistivity contour plot for Wenner array true model.....	68

Figure 4.2	Two-dimensional resistivity contour plots comparison between (a) true model, and estimated models for Wenner array using conventional program with one electrode offline (WN-1EO) at (b) 0.1 m, (c) 0.2 m, (d) 0.3 m, (e) 0.4 m, (f) 0.5 m, (g) 0.6 m (h) 0.7 m (i) 0.8 m (j) 0.9 m (k) 1.0 m (l) 1.1 m (m) 1.2 m distances respectively. The arrow sign indicate the position of the offline electrode	70
Figure 4.3	Two-dimensional resistivity contour plots comparison between (a) true model, and estimated models for Wenner array using conventional program with one offline electrode (WN-2EO) at (b) 0.2 m, (c) 0.4 m, (d) 0.6 m, (e) 0.8 m, (f) 1.0 m, (g) 1.2 m distances respectively. The arrow sign indicates the position of the offline electrode	72
Figure 4.4	Two-dimensional resistivity contour plots comparison between (a) true model, and estimated models for Wenner array using conventional program with one offline electrode (WN-2EO) at (b) 0.2 m, (c) 0.4 m, (d) 0.6 m, (e) 0.8 m, (f) 1.0 m, (g) 1.2 m distances respectively. The arrow sign indicates the position of the offline electrode	74
Figure 4.5	Two-dimensional resistivity contour plot for the true model using Wenner-Schlumberger array.	78
Figure 4.6	Two-dimensional resistivity contour plots comparison between (a) true model, and estimated models for Wenner-Schlumberger using the conventional program with one offline electrode (WN-1EO) at (b) 0.2 m, (c) 0.4 m, (d) 0.6 m, (e) 0.8 m, (f) 1.0 m, (g) 1.2 m distances respectively. The arrow sign indicates the position of the offline electrode	80
Figure 4.7	Two-dimensional resistivity contour plots comparison between (a) true model, and estimated models for Wenner-Schlumberger using the conventional program with one offline electrode (WN-2EO) at (b) 0.2 m, (c) 0.4 m, (d) 0.6 m, (e) 0.8 m, (f) 1.0 m, (g) 1.2 m	

	distances respectively. The arrow sign indicates the position of the offline electrode	82
Figure 4.8	Two-dimensional resistivity contour plots comparison between (a) true model, and estimated models for Wenner-Schlumberger using the conventional program with one offline electrode (WN-2EO) at (b) 0.2 m, (c) 0.4 m, (d) 0.6 m, (e) 0.8 m, (f) 1.0 m, (g) 1.2 m distances respectively. The arrow sign indicates the position of the offline electrode.	84
Figure 4.9	2-D resistivity processing template that enables incorporation of electrodes offline	88
Figure 4.10	2-D resistivity data using (a) conventional program (b) Innovative template	89
Figure 4.11	Two-dimensional resistivity contour plots comparison between (a) true model, and estimated models for Wenner array using conventional program and innovative template with one offline electrode (WN-1EO) at (b/b') 0.2 m, (c/c') 0.4 m, (d/d') 0.6 m, (e/e') 0.8 m, (f/f') 1.0 m, (g/g') 1.2 m distances respectively. The arrow sign indicates the position of the offline electrode	90
Figure 4.12	Two-dimensional resistivity contour plots comparison between (a) true model, and estimated models for Wenner array using conventional program and innovative template with two offline electrodes (WN-2EO) at (b/b') 0.2 m, (c/c') 0.4 m, (d/d') 0.6 m, (e/e') 0.8 m, (f/f) 1.0 m, (g/g') 1.2 m distances respectively. The arrow sign indicates the position of the offline electrode	91
Figure 4.13	Two-dimensional resistivity contour plots comparison between (a) true model, and estimated models for Wenner array using the conventional program and the innovative template with three offline electrodes (WN-3EO) at (b/b') 0.2 m, (c/c') 0.4 m, (d/d') 0.6 m, (e/e') 0.8 m, (f/f') 1.0 m, (g/g') 1.2 m distances respectively. The arrow sign indicates the position of the offline electrode	93
Figure 4.14	Two-dimensional resistivity contour plots comparison between (a) true model, and estimated models for Wenner-Schlumberger using	

the conventional program and innovative template with one offline electrode (WNS-1EO) at (b/b') 0.2 m, (c/c') 0.4 m, (d/d') 0.6 m, (e/e') 0.8 m, (f/f') 1.0 m, (g/g') 1.2 m distances respectively. The arrow sign indicates the position of the offline electrode97

Figure 4.15 Two-dimensional resistivity contour plots comparison between (a) true model, and estimated models for Wenner-Schlumberger array using conventional program and innovative template with two offline electrodes (WN-2EO) at (b/b') 0.2 m, (c/c') 0.4 m, (d/d') 0.6 m, (e/e') 0.8 m, (f/f') 1.0 m, (g/g') 1.2 m distances respectively. The arrow sign indicates the position of the offline electrode98

Figure 4.16 Two-dimensional resistivity contour plots comparison between (a) true model, and estimated models for Wenner-Schlumberger array using the conventional program and innovative template with two offline electrodes (WN-3EO) at (b/b') 0.2 m, (c/c') 0.4 m, (d/d') 0.6 m, (e/e') 0.8 m, (f/f') 1.0 m, (g/g') 1.2 m distances respectively. The arrow sign indicates the position of the offline electrode 100

LIST OF SYMBOLS

A	Electrode spacing
E	Electric field
I	Current
J	Current density
K	Geometrical factor
L	Length
M	Meter
N	Ratio of spacing between C and P
P	Potential electrode
R	Radius
R	Resistance
V	Voltage
Σ	Electrical conductivity
P	Resistivity
∇	Differential operator
°	Degree
Ωm	Ohm-metre
ΔV	Potential difference
ρ_a	Apparent resistivity
-	Minus
+	Plus
\pm	Plus or minus
π	Pi
%	Percentage

$>$	Greater than
\geq	Greater than or equal to
$<$	Less than
\leq	Less than or equal to

LIST OF ABBREVIATIONS

1-D	One-dimensional
2-D	Two-dimensional
3-D	Three-dimensional
AE	Absolute error
A-B	Current electrode pairs
D.C.	Direct current
DD	Dipole-dipole array
ERT	Electrical resistivity tomography
MAE	Mean absolute error
MAPE	Mean absolute percentage error
M-N	Potential electrode pairs
PCC	Pearson's correlation coefficient
PDP	Pole-dipole array
PP	Pole-pole array
Res2Dinv	Resistivity two-dimensional inversion
SAS 4000	Signal Averaging System 4000
USM	Universiti Sains Malaysia
VES	Vertical electrical sounding
WN	Wenner array
WNS	Wenner-Schlumberger array

LIST OF APPENDICES

- APPENDIX A RESISTIVITY DATA ACQUISITION EQUIPMENTS
- APPENDIX D RESISTIVITY CONTOUR PLOTS FOR WENNER ARRAY WITH TWO ELECTRODES OFFLINE AT ODD NUMBER DISTANCES (0.1, 0.3, 0.5, 0.7, 0.9, 1.1 M) USING CONVENTIONAL PROGRAM
- APPENDIX F RESISTIVITY CONTOUR PLOTS FOR WENNER ARRAY WITH THREE ELECTRODES OFFLINE AT ODD NUMBER DISTANCES (0.1, 0.3, 0.5, 0.7, 0.9, 1.1 M) USING CONVENTIONAL PROGRAM
- APPENDIX H RESISTIVITY CONTOUR PLOTS FOR WENNER-SCHLUMBERGER ARRAY WITH ONE ELECTRODES OFFLINE AT ODD NUMBER DISTANCES (0.1, 0.3, 0.5, 0.7, 0.9, 1.1 M) USING CONVENTIONAL PROGRAM
- APPENDIX J RESISTIVITY CONTOUR PLOTS FOR WENNER-SCHLUMBERGER ARRAY WITH TWO ELECTRODES OFFLINE AT ODD NUMBER DISTANCES (0.1, 0.3, 0.5, 0.7, 0.9, 1.1 M) USING CONVENTIONAL PROGRAM
- APPENDIX L RESISTIVITY CONTOUR PLOTS FOR WENNER-SCHLUMBERGER ARRAY WITH THREE ELECTRODES OFFLINE AT ODD NUMBER DISTANCES (0.1, 0.3, 0.5, 0.7, 0.9, 1.1 M) USING CONVENTIONAL PROGRAM
- APPENDIX B RESISTIVITY CONTOUR PLOTS FOR WENNER ARRAY WITH ONE ELECTRODE OFFLINE AT ODD NUMBER DISTANCES (0.1, 0.3, 0.5, 0.7, 0.9, 1.1 M) USING CONVENTIONAL PROGRAM AND INNOVATIVE TEMPLATE
- APPENDIX E RESISTIVITY CONTOUR PLOTS FOR WENNER ARRAY WITH TWO ELECTRODES OFFLINE AT ODD NUMBER DISTANCES (0.1, 0.3, 0.5, 0.7, 0.9, 1.1 M) USING CONVENTIONAL PROGRAM AND INNOVATIVE TEMPLATE
- APPENDIX G RESISTIVITY CONTOUR PLOTS FOR WENNER ARRAY WITH THREE ELECTRODES OFFLINE AT ODD NUMBER DISTANCES (0.1, 0.3, 0.5, 0.7, 0.9, 1.1 M) USING CONVENTIONAL PROGRAM AND INNOVATIVE TEMPLATE

APPENDIX I RESISTIVITY CONTOUR PLOTS FOR WENNER-SCHLUMBERGER ARRAY WITH ONE ELECTRODES OFFLINE AT ODD NUMBER DISTANCES (0.1, 0.3, 0.5, 0.7, 0.9, 1.1 M) USING CONVENTIONAL PROGRAM AND INNOVATIVE TEMPLATE

APPENDIX K RESISTIVITY CONTOUR PLOTS FOR WENNER-SCHLUMBERGER ARRAY WITH TWO ELECTRODES OFFLINE AT ODD NUMBER DISTANCES (0.1, 0.3, 0.5, 0.7, 0.9, 1.1 M) USING CONVENTIONAL PROGRAM AND INNOVATIVE TEMPLATE

APPENDIX M RESISTIVITY CONTOUR PLOTS FOR WENNER-SCHLUMBERGER ARRAY WITH THREE ELECTRODES OFFLINE AT ODD NUMBER DISTANCES (0.1, 0.3, 0.5, 0.7, 0.9, 1.1 M) USING CONVENTIONAL PROGRAM AND INNOVATIVE TEMPLATE

**KESAN ANJAKAN ELEKTROD TERHADAP SUSUNATUR WENNER DAN
WENNER-SCHLUMBERGER MENGGUNAKAN TOMOGRAFI
KEBERINTANGAN ELEKTRIK DUADIMENSI**

ABSTRAK

Susunatur piawaian yang digunakan untuk tinjauan tomografi keberintangan elektrik dua dimensi (2-D ERT) direka bentuk dengan anggapan bahawa pasangan elektrod kolinear pada setiap titik pengukuran. Namun, disebabkan oleh kekangan permukaan yang berkaitan dengan kebanyakan kawasan tinjauan, jarang sekali dapat menjalankan tinjauan resistiviti sepanjang garis lurus. Oleh itu, tinjauan 2-D ERT dijalankan di lapangan kekangan permukaan yang memerlukan anjakan beberapa elektrod dari luar garis tinjauan, yang berbeza dengan prinsip dasar. Akibatnya, ketidakpastian mungkin mempengaruhi hasil kajian. Tujuan penyelidikan ini adalah untuk mengenal pasti kesan potensi teraju dari elektrod-elektrod luar garisan kepada data keberintangan 2-D dan membangunkan templat untuk mengurangkan kesannya. Untuk tujuan ini, tomografi keberintangan menggunakan susunatur-susunatur yang paling biasa (Wenner dan Wenner-Schlumberger) telah dijalankan. Untuk setiap susunatur, data diperoleh dengan semua multi-elektrod sejajar, satu elektrod luar garisan, dua elektrod luar garisan, dan tiga elektrod luar garisan dengan jarak diubah secara berperingkat. Hasilnya menunjukkan bahawa elektrod-elektrod luar garisan tinjauan 2-D ERT mempunyai kesan yang ketara pada kedua-dua susunatur, terutamanya apabila dua atau lebih elektrod-elektrod berada luar garisan pada jarak $> \frac{1}{2}$ sela elektrod minimum "a". Juga, penilaian kuantitatif yang dilakukan menggunakan pekali korelasi Pearson (PCC), ralat mutlak purata (MAE), dan ralat peratusan mutlak purata (MAPE) selanjutnya menunjukkan kesan dengan PCC rendah

(<0.7). Walau bagaimanapun, ralat peratusan tinggi (>18%) untuk model susunatur Wenner-Schlumberger dan rendah (<10%) untuk model susunatur Wenner. Ini menunjukkan bahawa, jika pasangan elektrod-elektrod kolinear tidak dijamin untuk pengukuran, susunatur Wenner lebih diutamakan berbanding susunatur Wenner-Schlumberger. Sebagai tambahan, templat inovatif yang bertujuan untuk mengurangkan kesan elektrod luar garisan telah dibangunkan pada persekitaran Jupyter Notebook menggunakan bahasa pengaturcaraan Python. Keberkesanan templat inovatif dinilai dengan membandingkan hasil yang diperoleh menggunakan templat dengan program konvensional. Templat inovatif didapati sangat berkesan, kerana memberikan gambaran anggaran sasaran dengan ketepatan >90%. Oleh itu, disimpulkan bahawa elektrod luar garisan mempunyai kesan yang signifikan terhadap tinjauan 2-D ERT dan penggunaan templat inovatif yang dibangunkann sangat disarankan untuk mengelakkan salah tafsir.

OFF-LINE ELECTRODES' EFFECT ON A WENNER AND WENNER-SCHLUMBERGER ARRAY USING TWO-DIMENSIONAL ELECTRICAL RESISTIVITY TOMOGRAPHY

ABSTRACT

Standard protocols employed for two-dimensional electrical resistivity tomography (2-D ERT) survey are designed with the assumption of collinear electrode pairs at each point of measurement. However, due to the presence of surface constraints associated with most of the survey areas, it is seldom possible to conduct resistivity surveys along a straight line. Therefore, 2-D ERT survey conducted on a surface constraint field requires shifting some electrodes off the survey line, which is in contrast to the underlying principle. Consequently, uncertainties might creep into the results. The purpose of this research is to ascertain the potential effect posed by electrodes offline on a 2-D resistivity data and develop a template to mitigate the effect. To this end, resistivity tomography using the most common arrays (Wenner and Wenner-Schlumberger) were conducted. For each array, data was acquired with all multi-electrodes inline, one offline, two offline, and three offline at stepwise distances, respectively. The results show that electrodes offline on a 2-D ERT survey have a significant effect on both arrays, especially when two or more electrodes are offline at a distance $> \frac{1}{2}$ the minimum electrode spacing " a ". Also, the quantitative assessment carried out using Pearson's correlation coefficient (PCC), mean absolute error (MAE), and mean absolute percentage error (MAPE) further revealed the effect with low PCC (< 0.7). The percentage error is however, high ($> 18\%$) for Wenner-Schlumberger array model and low ($< 10\%$) for Wenner array model. This implies that, if collinear electrodes pair is not guaranteed for a 2-D ERT measurement, Wenner array is

preferred over Wenner-Schlumberger array. In addition, an innovative template meant to mitigate the offline electrodes effect had been developed on Jupyter notebook environment using Python programming language. The efficacy of the innovative template was evaluated by comparing the results obtained using the template to that of the conventional program. The innovative template was found to be very effective, as it provides an approximate representation of the target with an accuracy of >90%. Therefore, it is concluded that the offline electrode has significant effect on 2-D ERT survey and the use of the developed innovative template is strongly recommended to avoid misinterpretation.

CHAPTER 1

INTRODUCTION

1.1 Background

In a broad way, the science of geophysics is the application of physics principles to investigate the Earth, Moon, and planets (Reynolds, 2011). However, the term ‘geophysics’ is often used in a more restricted manner, being applied solely to the Earth (Kearey et al., 2002) known as ‘solid Earth geophysics.’ Traditionally, solid Earth geophysics is subdivided into global or pure geophysics, which is the study of the whole or substantial parts of the planet, and exploration geophysics, which is concerned with the investigation of the Earth’s crust and near-surface to achieve a practical and economic aim. The investigation is performed through conducting and interpreting measurements of contrast in the Earth’s physical properties to deduce its subsurface condition for a desired goal such as detection of subsurface structures, the discovery of mineral, groundwater or oil depositions (Sheriff, 2002).

The detection of subsurface structures, therefore, relies on those physical properties that distinguish them from the surrounding media. Different geophysical methods may thus be employed for subsurface investigation depending on their suitability to resolve target structures in relation to its surrounding environment. For instance, the gravity method is only efficient when there is a variation in density within the subsurface geology (Essa & Munsch, 2019; Uwiduhaye et al., 2018). The same goes for the magnetic method; it is useful when magnetic susceptibility contrast exists between the surrounding and the target materials (Ibraheem et al., 2018). In a similar vein, the seismic method focuses on the velocity contrast of acoustic waves as they travel through the subsurface to distinguish between rocks and soils of different materials (Adelinet et al., 2018). Ground Penetration Radar (GPR) is yet another

powerful geophysical method with conductivity as its measured physical property. It is used for very shallow studies, particularly when subsurface objects are distinguishable by their conductivity or reflectivity to radar pulse (Utsi, 2017).

Furthermore, the physical properties of interest for this research is the resistivity. Thus, the electrical resistivity method utilizes contrast in resistivity distribution to distinguish between subsurface structures (Papadopoulos et al., 2009). In this method, an electric current is injected into the ground through two current electrodes. Then, the electric potential is measured through another set of two electrodes. Since the amount of current supplied is known, it is, therefore, possible to calculate the effective subsurface resistivity. This attribute makes the method superior to all other electrical methods as quantitative results are obtained through the application of a controlled current source (Telford et al., 1990). Despite the above merits, the potentialities of the method are still under maximized, perhaps, due to its high sensitivity to minor changes in subsurface conductivity.

Electrical resistivity method has been used to solve practical problems such as in forensic studies (Reynolds, 2011), groundwater exploration (Kumar et al., 2020; Saad et al., 2012), engineering site characterization (Abudeif et al., 2020; Amini & Ramazi, 2016), mineral exploration (Moreira et al., 2019; Uhlemann et al., 2018), detection of underground cavities (Kolesnikov & Fedin, 2018) and shallow archaeological investigation (Papadopoulos et al., 2006). It has also been proved useful in the delineation of leachate plume migration (Ganiyu et al., 2015). This is feasible considering the rapid and progressive advancement of the method in terms of availability of forward modelling and inversion schemes, efficient data acquisition and processing techniques (Ingeman-Nielsen et al., 2016; Rucker et al., 2012)

Multi-electrode resistivity systems employed to resolve geophysical problems, use multi-core cables that connect to a series of electrodes at constant spacings. A switcher unit (Electrode Selector, ES 464) automatically selects two electrode pairs by which current is injected into the Earth, and the resulting electric potential difference is measured (Kiflu et al., 2016). The selected electrode pairs depend on the pattern of electrode arrangement commonly called electrode arrays (configurations), for example, Wenner (W), Schlumberger (S), Pole-dipole (PDP), Pole-pole (PP) and Dipole-dipole (DD) arrays (Lowrie, 2007; Telford et al., 1990). Of all the configurations, Wenner and Wenner-Schlumberger arrays are the most commonly used due to their high signal strength and sensitivity to vertical and horizontal changes (Cubbage et al., 2017; Muhammad & Saad, 2018), and they are employed for this study. Both arrays are designed with the assumption of four collinear electrodes arrangement at every point of measurement. However, with most of the survey areas been characterized by rocky field, thick vegetation, very rough terrain, and other surface constraints, it is seldom possible to conduct a two-dimensional electrical resistivity survey with all multi-electrodes in a straight line. This, therefore, poses a question on the reliability of results obtained using two-dimensional electrical resistivity tomography (2-DERT) in surface constraint field since there is non-conformity between the underlying theoretical principle of having four collinear electrodes and real field scenarios. Consequently, this research was initiated and conducted at Universiti Sains Malaysia (USM), Penang Island. The geological setting of the Island is relatively homogeneous where it is completely made up of granitic rocks (Kong, 1994). Evidence from the borehole log information of USM shows that the area consists largely of residual soil (Abdulrahman et al., 2016). The residual soil composed of silt and/or clayey sand which spans to a depth of about 15 m from the

surface. More so, the study area has a shallow water table mostly at 2.7 m depth (Abdulrahman et al., 2016).

1.2 Problem statements

Two-dimensional electrical resistivity tomography (2-DERT) remains the most commonly used geophysical method to image the subsurface due to its simplicity (in terms of data acquisition and processing) and cost-effectiveness (Dahlin & Zhou, 2004). Multi-electrode resistivity systems, such as Lund Imaging System, used for 2-DERT, employ standard protocols for data acquisition. Theoretically, these protocols, assumed that the survey lines are straight to ensure collinearity between the various electrode pairs at each point of measurement (Loke et al., 2013). More so, the conventional software to process the 2-D ERT data are built with the same assumptions. Thus, all calculations done during the processing are based on those assumptions.

However, in practice, such collinearity of the multi-electrodes is rarely possible due to surface constraints (thick vegetation, rough terrain and rocky fields) of which most survey areas are characterized with. Therefore, 2-D ERT survey conducted on a surface constraint field requires shifting of some electrodes off the survey line, which implies a non-collinear electrodes arrangement. In this light, uncertainties might creep into the result, which could lead to false interpretation. To this end, Zhou & Dahlin (2003) investigated the properties and effect of measurement error (off-line and in-line spacing error) on 2-D resistivity tomography survey. In their study, the offline electrodes causing the offline spacing error were omitted. Hence, they concluded that the in-line spacing errors are much larger than the offline spacing error. In a similar work by Szalai *et al.* (2008) found that the electrode positioning error is insignificant

except for a very rocky field. They suggested neglecting a few position errors with the greatest positioning error to be the possible solution. However, ignoring some electrodes could jeopardise the quality of the data and thus, imperil the correct interpretation. Hence, the need to ascertain the effect of the electrode(s) offline on a 2-D electrical resistivity profile and possibly develop a pre-processing template for a non-collinear two-dimensional resistivity profile.

1.3 Research objectives

The specific objectives of the research are as follow;

- i. To ascertain the effect of the electrode(s) offline on a 2-D electrical resistivity tomography profile.
- ii. To develop an innovative processing template that could mitigate the effect of the offline electrode(s) on a 2-D ERT survey.
- iii. To evaluate the effectiveness of the innovative template and compare its performance with the conventional program.

1.4 Scope of study

The focus in this study is to ascertain the effect of the offline electrode(s) on a two-dimensional electrical resistivity tomography profiles, determine the optimum distance to which an offline electrode can be shifted and to develop a template that could mitigate the effect. Only two arrays; Wenner and Wenner-Schlumberger were considered because they are the most commonly used arrays (Rinaldi et al., 2006). All the electrodes offline are shifted perpendicularly off the survey line throughout this research. The study was conducted at Universiti Sains Malaysia, Pulau Pinang, Malaysia. Prior to the study, some preliminary resistivity profiles were taken with

reference to the borehole record which shows that the area is composed of residual soil of uniform composition, thus, makes it suitable for this study.

Lund imaging system (ABEM SAS 4000 Terrameter) was used to acquire the data. The data processing, visualization and analysis were performed using Res2Dinv, Surfer 13 and Microsoft excel respectively. In addition, Python programming language was used for the template development.

1.5 Significance and novelty of the study

This research seeks to make known the effect of the electrode(s) offline on a two-dimensional electrical resistivity tomography survey using Wenner and Wenner-Schlumberger array. A significant variation was observed for the survey with some electrodes offline when compared to the survey with all electrodes inline. The research has created great awareness for the 2-D ERT practitioners with regards to the reliability of the data when some electrodes are offline.

The main novelty of this research is that the study is the first of its kind to make known the potential effect of electrodes offline on a two-dimensional resistivity tomography survey. The research redefined the existing geometric factor equation for arrays under consideration to address the non-collinear electrode arrangement. It is also the first to develop and evaluate an innovative processing template that could mitigate the effect of offline electrodes on a 2-D ERT survey.

1.6 Thesis layout

The layout of this thesis is organized as follows:

Chapter one is the introductory chapter, in which the general summary of this research framework is provided. Starting with the background of this research to the

problem statement, scope and objectives of the research. The significant and novelty as well as the thesis layout are presented.

Chapter two presents a detailed review of the application of two-dimensional electrical resistivity tomography in addressing geological, engineering, and environmental problems. In the review process, the lacuna, which forms the basis of this research, is highlighted.

Chapter three discussed the research methodology in this study. A concerted effort was devoted to discussing the fundamental concepts and theoretical framework of the electrical resistivity method. Then, the electrode arrangements for data acquisition of the conventional arrays are highlighted. The methodology designed to achieve these research objectives is explained and illustrated. Data acquisition and processing for the selected arrays are also highlighted. The steps used to carry out the quantitative assessment and develop the new processing template that will account for the offline electrode(s) in a two-dimensional electrical resistivity profile are presented. Also, the geology of the study area is described.

Chapter four is dedicated to the result and discussions of the research findings according to the designed methodology. It starts with a qualitative assessment of the effect of the offline electrode(s) on 2-D electrical resistivity tomography profiles based on the inverse resistivity models using Res2Dinv software. Then, the optimum distance that an electrode(s) can be offline without significant effect. The numerical/quantitative assessment result for the inline survey and survey with offline electrodes are presented. The qualitative and quantitative comparisons are made between the two selected arrays in terms of the offline electrode(s) effect. More so, an innovative processing template had been developed and tested using Python

programming language. The effectiveness of the template is assessed by comparing its result to that of the conventional program.

Chapter five contains the conclusion, which summaries the major findings of this research and recommendation for future work.

CHAPTER 2

LITERATURE REVIEW

2.1 Introduction

This chapter provides an overview of the basic principle of the electrical resistivity method. The concept of two-dimensional electrical resistivity tomography, its survey procedure, the commonly used electrodes array and their characteristics are presented. Relevant literature of surveys using 2-D ERT is also presented.

The electrical resistivity method is one of the oldest and most commonly used geophysical survey methods (Dahlin, 2001; Loke, 1999). Since resistivity is one of the most variable physical properties of Earth materials (rocks and minerals) (Figure 3.1), the method is likely to be more sensitive to subsurface variation than other geophysical techniques. As a result of this and other factors such as its conceptual simplicity and cost-effectiveness, the method is widely and increasingly applied in groundwater and mineral exploration, archaeological mapping, as well as environmental and engineering problems (Dahlin & Zhou, 2004; Zhou, 2018). The method involves injecting artificially generated electric current into the ground through a pair of electrodes and observing the resulting potential difference through the other pair of electrodes. The measured potential differences are then transformed into sounding curves of apparent resistivities, which indicate the resistivity variations of subsurface Earth materials (Zhou, 2018). Analyses of these data reveal the underground resistivity anomalies or the subsurface geological structure.

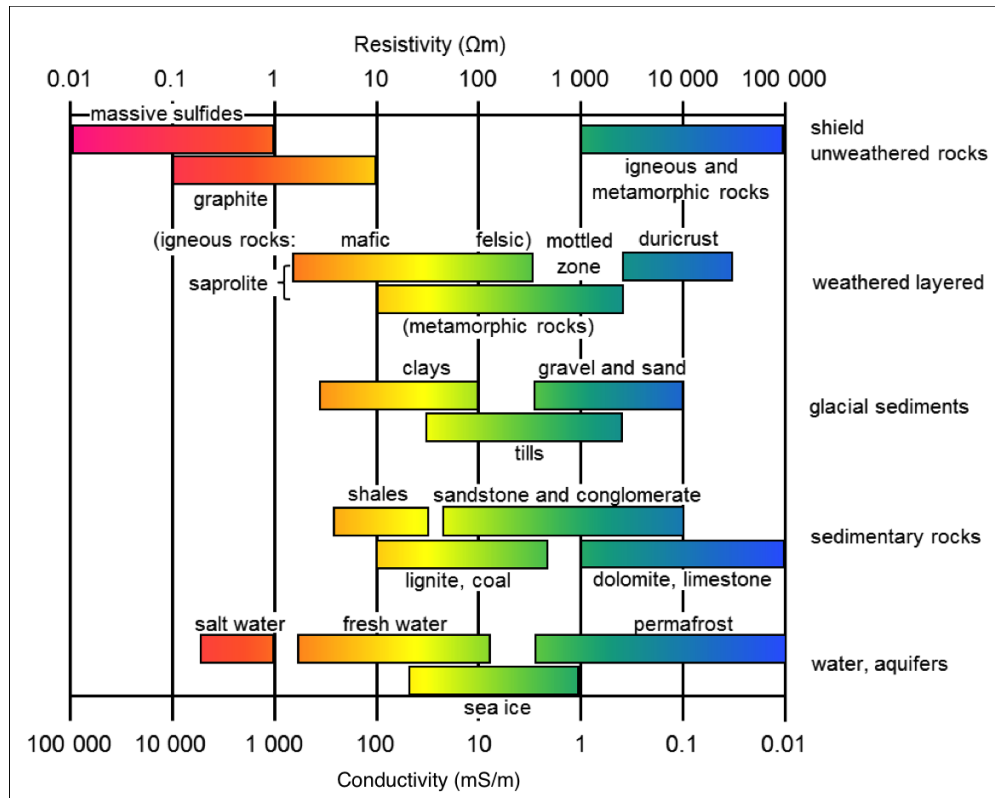


Figure 2.1 Resistivity value of some common Earth materials (Palacky, 1987)

2.2 The basic theory of the resistivity method

The fundamental physics principle governing the resistivity method is embodied in Ohm's Law, which states that the electric current, I in a conducting medium, is directly proportional to the potential difference, V across the conductor. The Law can be expressed mathematically by Equation 2.1;

$$V = IR \quad (2.1)$$

where R = resistance of the medium in ohms (Ω)

I = electric current in ampere (A)

V = potential difference/voltage in volt (V)

It can be stated alternatively as the current density at a given point is proportional to the electric field intensity at that point. Thus, Ohm's Law provides the

relationship between current density, J (Amperes per square meters) and electric field intensity, E (volts m) as in Equation 2.2;

$$J = \sigma E \quad (2.2)$$

where σ is the electrical conductivity of the medium in siemens per meter (S/m).

The electric field, E in Equation 2.3 is defined by the gradient of the electric potential function, ∇V ;

$$E = -\nabla V \quad (2.3)$$

Substituting Equation 2.3 into Equation 2.2 to produce current density as Equation 2.4;

$$J = -\sigma \nabla V \quad (2.4)$$

From divergence condition (in a charge-free zone), $\nabla \cdot J = 0$, as Equation 2.5;

$$\nabla \cdot J = -\nabla \cdot (\sigma \nabla V) = 0 \quad (2.5)$$

Applying vector operator, ∇ to the product $\sigma \nabla V$, σ being a scalar function as Equation 2.6;

$$\nabla \sigma \cdot \nabla V + \sigma \nabla^2 V = 0 \quad (2.6)$$

For an isotropic homogeneous medium, σ is a constant. Hence, Equation 3.6 reduces to Equation 2.7;

$$\nabla^2 V = 0 \quad (2.7)$$

Equation 2.7 is called Laplace's equation, where ∇^2 is a second derivative operator, and V is the potential. The equation can be solved by satisfying two boundary conditions; the electric field tangential to the interface must be continuous, and the current density normal to the interface must also be continuous.

Consider the scenario where a single point current electrode installed in a homogeneous isotropic medium and the second current electrode needed to make a complete circuit is far away (at infinity) that its effect is insignificant (Figure 2.2). In

this situation, the current flows radially away from the current electrode (source), and it is orthogonal to the equipotential surface.

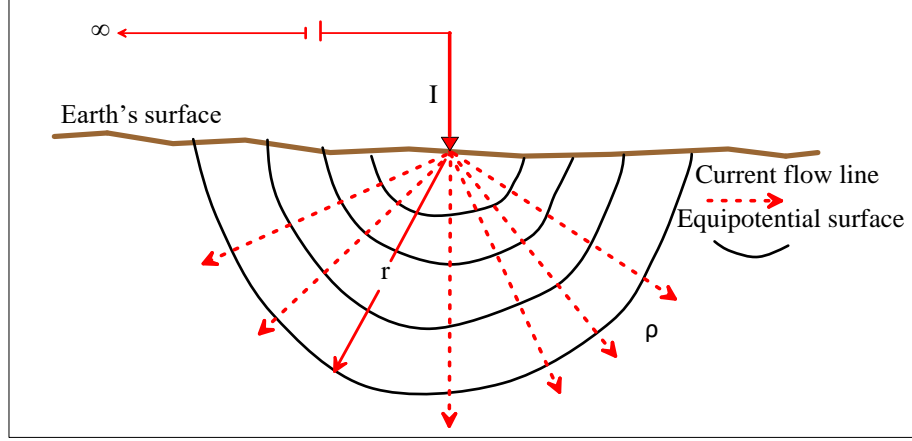


Figure 2.2 Current flow a single-point current electrode (Modified from Kearey et al., 2002)

The measured potential is a function of distance (r) from the current electrodes. Based on the spherical symmetry in the homogeneous subsurface, the potential will only be a function of the distance from the current electrode source. Hence, Equation 2.7 can be expressed in spherical coordinate as Equation 2.8;

$$\nabla^2 V = \frac{1}{r^2} \frac{\partial}{\partial r} \left(r^2 \frac{\partial V}{\partial r} \right) + \frac{1}{r^2 \sin^2 \varphi} \left(\frac{\partial^2 V}{\partial \theta^2} \right) + \frac{1}{r^2 \sin \varphi} \frac{\partial}{\partial \theta} \left(\sin \varphi \frac{\partial V}{\partial \varphi} \right) = 0 \quad (2.8)$$

For a point current source, there is complete symmetry of current flow with respect to θ and φ directions. Thus, the derivatives with respect to these directions are zero. Thus, Equation 2.8 reduces to Equation 2.9;

$$\nabla^2 V = \frac{d}{dr} \left(r^2 \frac{dV}{dr} \right) = 0 \quad (2.9)$$

Integrating Equation (2.9) to produce Equation 2.10;

$$r^2 \frac{dV}{dr} = C \quad (2.10)$$

Integrating Equation 2.10 produces Equation 2.11;

$$V = -\frac{C}{r} + D \quad (2.11)$$

where C and D are constant, V is the electric potential measured at a given point, and r is the distance from that given point the current electrode (source). Since, $V = 0$ as $r \rightarrow \infty$, then the $D = 0$. Hence Equation 2.11 reduces to Equation 2.12;

$$V = -\frac{C}{r} \quad (2.12)$$

Moreover, the current flows from the source electrode radially outwards and is perpendicular to the hemisphere-shaped equipotential surface. Therefore, the total current crossing the hemisphere of radius r shows as Equation 2.13;

$$I = 2\pi r^2 J \quad (2.13)$$

Putting Equation 2.4 into Equation 2.13 and simplify to get current, I as Equation 2.14;

$$I = -2\pi r^2 \sigma \frac{dV}{dr} = -2\pi \sigma C = -\frac{2\pi C}{\rho} \quad (2.14)$$

Rearranging Equation 2.14 to the form of Equation 2.15;

$$C = -\frac{I\rho}{2\pi} \quad (2.15)$$

Substituting Equation 2.15 into Equation (2.12) to get relation for the potential as Equation 2.16;

$$V = \frac{I\rho}{2\pi r} \quad (2.16)$$

Equation 2.16 can be rearranged to obtain the apparent resistivity as Equation 2.17;

$$\rho = \frac{2\pi r V}{I} \quad (2.17)$$

However, in a real field situation, all resistivity surveys require at least two current electrodes with a finite distance between them. Figure 2.3 shows that the electric flux around a source electrode which injected current into the Earth is radially outward,

while for the sink electrode through which current flows out of the Earth, the flux is directed radially inward (Lowrie, 2007; Van Nostrand & Cook, 1966). Hemispherical equipotential surfaces are formed around the two-point current electrodes (source and sink electrodes). Both current electrodes tend to affect the potential at any nearby surface point.

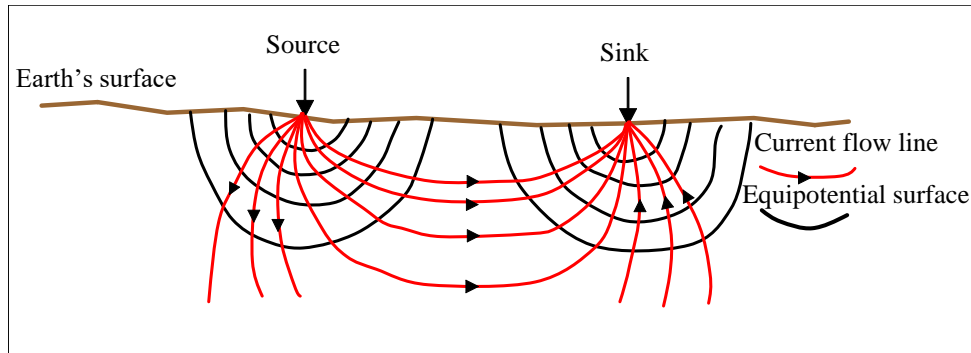


Figure 2.3 Current lines and equipotential surfaces produced by a current source and sink (modified from (Lowrie, 2007))

In general, for all electrical resistivity surveys, the potential difference between two points is measured. Figure 2.4 shows the arrangement of the electrodes, consisting of pairs of current and potential electrodes used to measure the potential difference. The current electrodes labelled C_1 and C_2 represent the source and sink respectively, while P_1 and P_2 represent the potential electrodes.

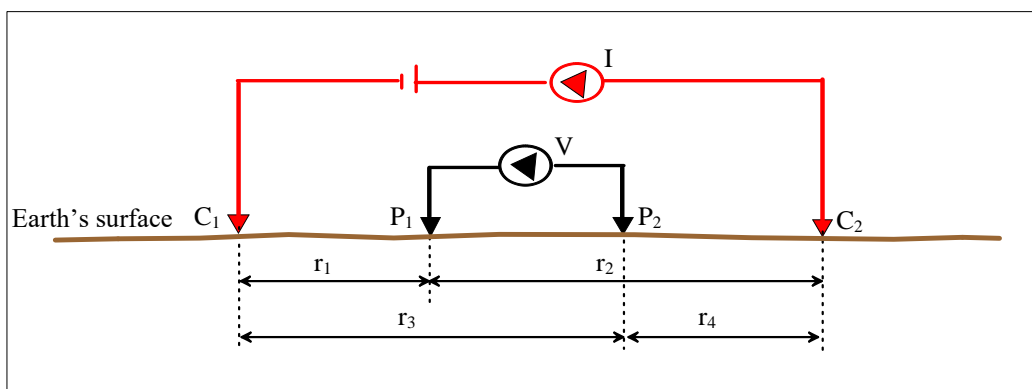


Figure 2.4 The general form of an electrode configuration for resistivity measurement (modified from Reynolds, 2011)

The potential at P_1 due to C_1 is as Equation 2.18;

$$V_1 = -\frac{C_1}{r_1} \quad (2.18)$$

$$\text{where } C_1 = -\frac{I\rho}{2\pi}$$

Since the current at the two electrodes are equal and opposite in direction, the potential at P_1 due to C_2 is as Equation 2.19;

$$V_2 = -\frac{C_2}{r_2} \quad (2.19)$$

$$\text{where } C_2 = \frac{I\rho}{2\pi} = -C_1$$

Therefore, adding Equation 3.18 and 3.19 yield the resultant potential at P_1 due to C_1 and C_2 as in Equation 2.20;

$$V_1 + V_2 = V_{P_1} = \frac{I\rho}{2\pi} \left(\frac{1}{r_1} - \frac{1}{r_2} \right) \quad (2.20)$$

Similarly, the resultant potential at P_2 due to C_1 and C_2 can be written as Equation 2.21;

$$V_{P_2} = \frac{I\rho}{2\pi} \left(\frac{1}{r_3} - \frac{1}{r_4} \right) \quad (2.21)$$

Consequently, the potential difference (ΔV) between two potential electrodes P_1 and P_2 can be measured as in Equation 2.22;

$$\Delta V = \frac{I\rho}{2\pi} \left\{ \left(\frac{1}{r_1} - \frac{1}{r_2} \right) - \left(\frac{1}{r_3} - \frac{1}{r_4} \right) \right\} \quad (2.22)$$

If the following parameters; current (I), potential difference (ΔV) and the inter-electrode distances r_1, r_2, r_3 and r_4 are known, then the resistivity can be determined using Equation 2.23, otherwise referred to as apparent resistivity (ρ_a) due to the heterogeneous nature of the Earth.

$$\rho_a = \frac{2\pi\Delta V}{I} \frac{1}{\left(\frac{1}{r_1} - \frac{1}{r_2} - \frac{1}{r_3} + \frac{1}{r_4} \right)} \quad (2.23)$$

where,

$$K = \frac{2\pi}{\left(\frac{1}{r_1} - \frac{1}{r_2} - \frac{1}{r_3} + \frac{1}{r_4}\right)} \quad (2.24)$$

K is called the geometric factor define for several electrode arrays configuration. The K factor depends on the arrangement of the four electrodes. Thus, the measured apparent resistivity dependent upon the geometry of the adopted electrode array (Kearey et al., 2002). Putting Equation 2.24 into Equation 2.23 to get Equation 2.25;

$$\rho_a = K \frac{\Delta V}{I} \quad (2.25)$$

Equation 2.25 can also be written in the form of Equation 2.26 if Equation 2.1 is substituted into Equation 2.25

$$\rho_a = KR \quad (2.26)$$

In practice, Equation 2.26 is used to calculate the apparent resistivity value. This calculated apparent resistivity is required to be transformed to obtain the true subsurface resistivity. Though the transformation is somewhat complex, it involves the inversion program through which true subsurface resistivity is generated from the apparent resistivity (Loke, 2000).

With the advancement of technology, the traditional direct current (DC) resistivity method has been transformed to a computerized geo-imaging method, called electrical resistivity tomography (ERT) where two dimensional (2-D) or three dimensional (3-D) surveys can be conducted using a multi-electrode system to automatically acquire a large number of data (Sasaki, 1992; Zhe et al., 2007). In practice, the outcome of the 3-D resistivity survey and interpretation is expected to be more accurate. However, until now, a 2-D resistivity survey remains the most realistic economic compromise between obtaining reliable results and ensuring low survey costs

(Dahlin, 1996; Loke, 2018). Hence, this research focus on the two-dimensional electrical resistivity tomography (2-D ERT).

To date, 2-D ERT survey remains the most common geophysical technique used for contamination monitoring (Bichet et al., 2016; Hu et al., 2019; Konstantaki et al., 2015), groundwater exploration (Attwa & Ali, 2018; Saad et al., 2012), archaeological investigation (Muztaza et al., 2014; Saad et al., 2014; Yogeshwar et al., 2019), subsurface cavity detection (Drahor, 2019; Park et al., 2014), landslide studies (Bellanova et al., 2016; Colangelo et al., 2008; Crawford et al., 2018) and subsurface characterization (Abudeif et al., 2020; Muztaza et al., 2012). This popularity of the method is attributed to its capabilities of multi-electrode data acquisition and availability of forward modelling and inversion scheme (Abdullah et al., 2018).

2.3 Concept of 2-D electrical resistivity tomography

Generally, at any given point for all resistivity surveys, measurements are carried out using a four-electrode system (pairs of current and potential electrodes). Two-dimensional resistivity imaging system utilizes an array of electrodes (usually 25 to 100) connected by multicore cables to provide a pseudo-section of the change in subsurface resistivity distribution, both along the survey line (laterally) and with depth (vertically). However, only four electrodes are used for each measurement at a point. The switching of the appropriate pairs of current and potential electrodes is automated using a programmable microprocessor within the resistivity meter (Loke et al., 2013). The above system speeds up data acquisition. Several electrode arrays with different geometry can be deployed to a survey using a multi-electrode system. For each configuration, an electrode sequence address file is installed to the instrument (resistivity meter) through a personal computer (PC). The information contained in the

address file, enable the device to inject current and measure potential difference through the designated electrodes depending on the geometry of the electrode array.

Figure 2.5 depicts a typical setup for a 2-D resistivity survey using a multi-electrode system; the separation between adjacent electrodes must be constant throughout a given survey line irrespective of the expected resolution, and target depth. Although the separation between the current and the potential electrodes depends on the type of electrode array, this separation is controlled automatically by the instrument based on the installed array protocol. The sequence of measurements is made along the survey line with different spacing between the electrodes, as shown in Figure 3.5. The first data level represents the measured data obtained from the first (minimum) electrode spacing. As the spacing between the electrodes increases, subsequent data levels are measured. This process continues until the maximum spacing between the electrodes is attained. A 2-D pseudo-section, which depicts the lateral and vertical resistivity distribution of the subsurface, is then obtained based on the measured data (Loke, 2018).

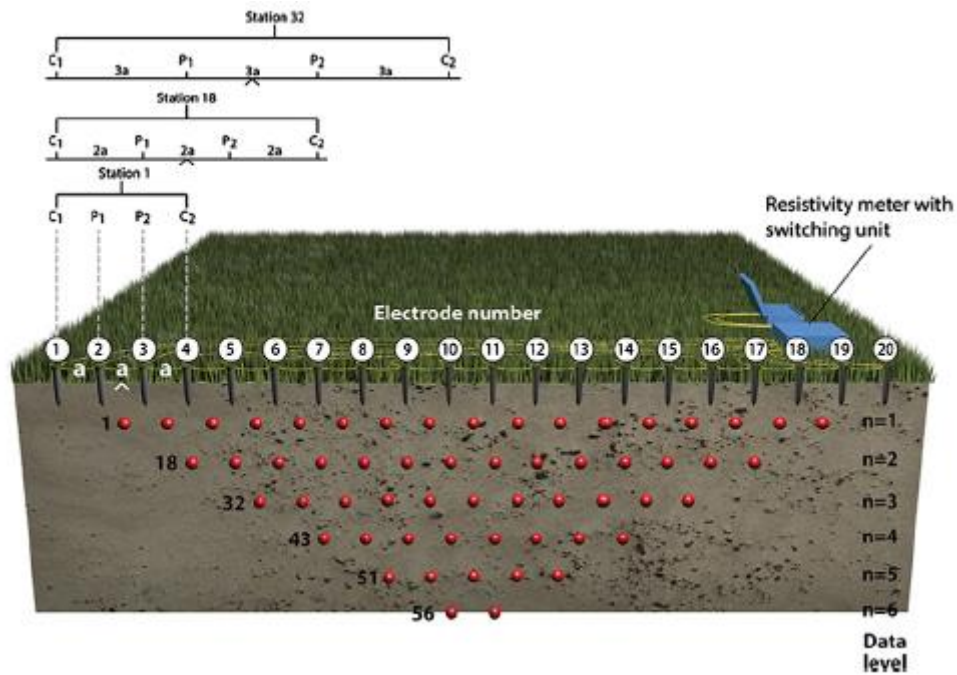


Figure 2.5 Electrode arrangement in a multi-electrode system for a 2-D resistivity survey and the measurement sequence used to construct a 2-D pseudo-section (Loke et al., 2013)

The effectiveness of 2-D resistivity imaging in subsurface investigations depends on the choice of appropriate electrode array configuration. Among the several electrode arrays, the most common and widely used in electrical resistivity surveys are Wenner (WN), Wenner-Schlumberger (WNS) and Dipole-Dipole (DD) (Sharma, 1997; Storz et al., 2000; Telford et al., 1990). Others include; pole-pole (PP), pole-dipole (PDP), and gradient (GRD) arrays (Eissa et al., 2019; Loke, 2018). The distinction between these types of configurations lies in the arrangement of the electrodes which provides a varying geometric factor for each electrode array. Moreover, each of the arrays has different characteristics such as sensitivity to vertical and lateral variations in the subsurface resistivity, horizontal data coverage, depth of investigation, and signal strength, which are subject of consideration while choosing an array. These arrays are briefly discussed in the following subsections.

2.3.1 Wenner array

Wenner array is one of the most commonly used configurations in electrical resistivity surveys for subsurface investigations. The array gains this versatility due to the simplicity of its geometry. In a Wenner array, the four electrodes are collinear with equidistance separation between adjacent electrodes (Figure 2.6). This separation is denoted by “a” which implies $r_1 = r_4 = a$ and $r_2 = r_3 = 2a$, as shown in Figure 2.4.

Substituting these notations into Equation 2.24 will yield, $K = 2\pi a$. The apparent resistivity in Equation 2.25, can now be rewritten as Equation (2.27) representing the measurement for Wenner array.

$$\rho_a = 2\pi a \frac{\nabla V}{I} \quad (2.27)$$

Where;

ρ_a = apparent resistivity

a = distance between adjacent electrodes

∇V = measured voltage (V)

I = current injected (mA).

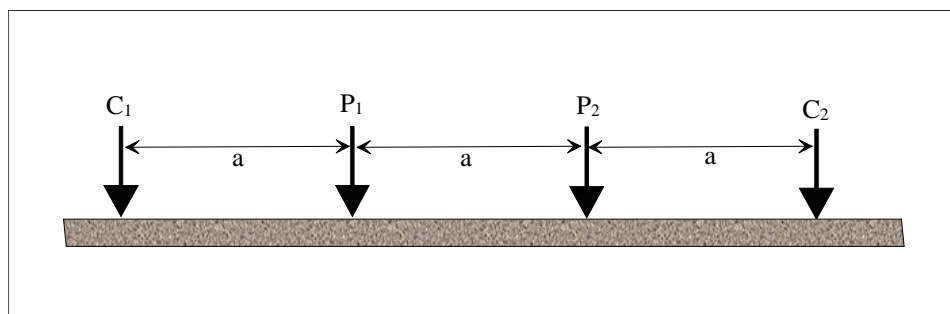


Figure 2.6 Electrodes arrangement for Wenner array

Wenner array can be used for both electrical sounding and profiling. In electrical sounding, the distance, “a” between the adjacent electrodes is increased stepwise with respect to the target depth of investigation, while keeping the mid-point of the array

fixed. In the case of profiling or electrical trenching, the four electrodes are moved horizontally in line throughout the survey line, while maintaining constant electrode separation (Herman, 2001). The measured apparent resistivity values for both cases are plotted against the spread specified by a horizontal position.

For a two-dimensional survey using Wenner array, the sounding and profiling are integrated into one system, and measurements are conducted simultaneously (Milsom, 2003). Wenner array has the strongest signal strength due to its small geometric factor, which is an essential parameter for survey areas with high background noise. It is quite sensitive to vertical variations of subsurface resistivity distribution below the centre of the array. However, it is less sensitive to horizontal changes in the subsurface resistivity distribution. Therefore, it is good at detecting horizontal subsurface structures but relatively poor in resolving vertical structures (Loke, 2007).

2.3.2 Schlumberger array

Schlumberger array is also one of the most frequently used arrays for subsurface studies. It is referred to as a symmetrical array (Figure 2.7), where $x = 0$ and $L > 10l$ (Sharma, 1997). Schlumberger array, like Wenner array, consists of four collinear electrodes. In this array, the outer two electrodes are current electrodes, and the inner two electrodes are potential electrodes. The apparent resistivity of this array is given as Equation 2.28;

$$\rho_a = \frac{\pi L^2 \nabla V}{I \ 2l} \quad (2.28)$$

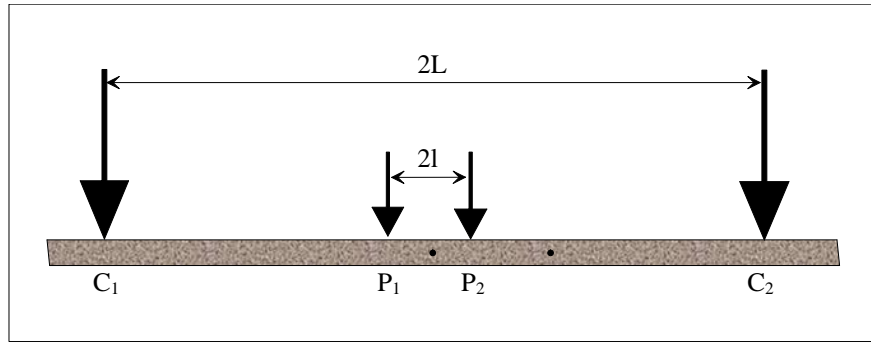


Figure 2.7 Electrodes arrangement for Schlumberger array

The apparent resistivity measurements are made by keeping the potential electrodes fixed about the midpoint of the array while the separation between the current electrodes C_1 and C_2 is increased systematically in steps during the survey. This array is moderately sensitive to both horizontal and vertical changes in the subsurface resistivity. Its signal strength is smaller than that of the Wenner array but is higher than the dipole-dipole array. The array provides better resolution when it is used to conduct a vertical electrical sounding survey (Keller, 1996).

2.3.3 Wenner-Schlumberger array

As the name implies, Wenner-Schlumberger (WS) array is the amalgamation between the Wenner and Schlumberger arrays (Loke, 2016; Pazdirek & Blaha, 1996). The array is designed such that it can be used on a multi-electrode system with electrodes arranged at constant spacing “ a ” (Figure 2.8). The “ n ” factor in this array represent the ratio of separation between C_1 and P_1 or $(C_2 - P_2)$ to the distance between the $P_1 - P_2$. Thus, the geometric factor “ K ” of this array depends upon the “ n ” factor and the “ a ” electrode spacing. Analyzing Figure 3.8 with reference to Figure 2.4 gives, $r_1 = r_4 = na$ and $r_1 = r_4 = (a + na)$. Inserting these notations into Equation 2.24 gives $K = \pi n(n + 1)a$. Therefore, the apparent resistivity from Equation 2.25 can written as Equation 2.29 for Wenner-Schlumberger (Loke, 2000).

$$\rho_a = \pi n(n + 1)a \frac{\nabla V}{I} \quad (2.29)$$

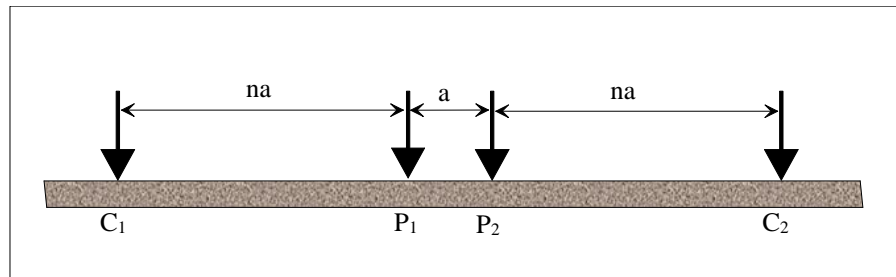


Figure 2.8 Electrodes arrangement for Wenner-Schlumberger array

The signal strength of WS array is smaller than that of Wenner array but stronger than that of Schlumberger array. Its median depth of investigation is about 10 % greater than that of Wenner array for the same separation between the current electrodes, C_1 and C_2 (Loke, 2018). In addition, the array is moderately sensitive to both horizontal and vertical changes in the subsurface resistivity. This makes it suitable for use in areas where both types of geological structures are of interest, as it might be of a good compromise between the Wenner and the dipole-dipole arrays. It also has a relatively better horizontal data coverage than the Wenner array, though smaller than the dipole-dipole array.

2.4 Measurement error in 2-D ERT survey

Several geophysical studies have been conducted using two-dimensional electrical resistivity tomography (2-D ERT) method. Most of these studies focus on the application of the method for subsurface investigation thereby ignoring the fundamental principle. It is important to note that most of the standard electrodes arrays employed for the 2-D ERT survey are designed with the theoretical assumption that the survey lines are straight to ensure collinear electrode pairs at each point of measurement. However, due to surface constraints which most survey areas are characterized with, it

is rarely possible to conduct 2-D ERT on a straight line. This could, therefore, leads to error in the 2-D ERT measurement and thus misinterpretation of the result. To this end, Zhou & Dahlin, (2003) investigated the properties and effect of measurement error (inline and offline spacing error) on a two-dimensional electrical resistivity tomography survey for all common electrodes arrays (Wenner, Wenner- β , Schlumberger, Pole-dipole, Pole-pole, dipole-dipole, pole-bipole, γ -array) They found that the magnitude of the spacing error depends on the type of array, with Wenner- β , dipole-dipole and γ -array having the largest error on the observed apparent resistivities which in turn produce some artefacts in the inverted model. More so, the inline spacing errors are much larger than the offline spacing error. This conclusion is based on the fact that the inline spacing error assumed that some selected electrodes have 10% negative or positive x position error relative to the basic spacing error of 1 m, whereas, the offline spacing error assumed that those selected electrodes were omitted. However, omitting some electrodes could jeopardize the quality of the data.

In a similar work, Szalai et al. (2008) conducted a survey to assess the effect of electrode positioning error on the inverted pseudo-section of a 2-D electrical resistivity tomography. Laser distance meter was used to measure the exact position inaccuracies of the electrodes. They concluded that the position error is insignificant in most cases (even in a field with varied topography). For the case where it is significant, neglecting a few electrode positions with the greatest positioning error is recommended. This could, however, makes the result to be subjective thereby affect the correct interpretation.

2.5 Evaluation of electrode arrays efficiency

The success of a 2-D electrical resistivity survey partly depends on the correct choice of the electrode array. The choice of the best array depends on different factors such as; depth of investigation, resolution, sensitivity and vertical and horizontal coverage. Quite a number of study have been carried out to evaluate the efficiency of the electrode arrays. However, virtually all the work tend to ignore the effect of varied topography and other surface constraints which could hinder having a collinear electrode pair, thereby contravene the theoretical assumption upon which the arrays are built. For instance (Dahlin & Zhou, 2004) used numerical simulation to compare the resolution and efficiency of 2-D resistivity tomography for some common electrode arrays (Wenner- α (WA), Wenner- β , (WB), half-Wenner (HW), Schlumberger (SC), pole-pole (PP), pole-dipole (PD), dipole-dipole (DD), γ -array (GA) and moving gradient (MG) arrays. The resistivity modelling software used for the simulation was built based on the theoretical assumption of having collinear electrode pairs at each point of measurement. They found that WA and GA are less contaminated with noise than the other arrays. They strongly recommend the use of SC, DD, PD and MG arrays for 2-D electrical resistivity tomography. However, for a practical case, these outcomes could differ because most of the survey areas are characterized by surface constraints which could impede having collinear electrode pairs, thereby contravening the theoretical assumption. Consequently, the correct interpretation could be impeded.

AL-Hameedawi & Thabit, (2017) performed a comparison between four electrodes arrays in delineating sedimentary layers of alluvial fan deposits using a 2-D ERT method. The array analysed include Wenner, Wenner-Schlumberger, Schlumberger reciprocal and Dipole-dipole. They concluded that the Wenner-Schlumberger array yields the optimal results corresponding to the deep subsurface